BIOMARKERS, VOL. 9, NO. 1 (JANUARY–FEBRUARY 2004), 32–46

Taylor & Francis
healthsciences

Biomonitoring of chromium(VI) deposited in pulmonary tissues: pilot studies of a magnetic resonance imaging technique in a post-mortem rodent model

ROB SHAYER[1], PAUL KINCHESH[2], MARK RAFFRAY[3] and ANDREAS KORTENKAMP[4]*

[1] Department of Health, Tobacco Policy Team, Wellington House, 133–155 Waterloo Road, London, SE1 8UG, UK
[2] Department of Medical Physics and Bioengineering, University College London, Shropshire House, 11–20 Capper Street, London, WC1E 6JA, UK
[3] FMC Toxicology 40/822, Station Way, Basildon, Essex, SS16 5XX, UK
[4] Centre for Toxicology, The School of Pharmacy, 29–39 Brunswick Square, London, WC1N 1AX, UK

Received 18 June 2003, revised form accepted 11 December 2003

The biomonitoring of individuals exposed to chromium(VI) by inhalation is often based on determinations of chromium in body fluids such as blood, plasma or urine, or on assessments of DNA damage in non-lung surrogate tissues such as peripheral blood lymphocytes. These techniques are of some use as biomarkers of internal exposure or biological effect, mainly in the case of soluble chromium(VI) compounds, but they provide at best only indirect information about chromium(VI) concentrations in the main target organ of interest – the lung. An urgent need exists for a non-invasive technique to permit the visualization and quantification of chromium(VI) in the lung of exposed humans. This study details the development of a lung imaging technique based on the detection of paramagnetic chromium using magnetic resonance imaging (MRI). The intracellular reductive conversion of chromium(VI) is a crucial bioactivation step in its carcinogenicity, and the MRI method described here relies on the conversion of non-paramagnetic (MRI 'silent') chromium(VI) to detectable paramagnetic species such as chromium(III). Initial studies with chromium(III) revealed that a range of 2.5–5 μg chromium(III) instilled in rat lung is considered to be the lower limit of detection of this method. It was possible to demonstrate the presence of 30 μg chromium(VI) in our post-mortem rat model. The ultimate objective of this work is to determine whether this technique has applicability to the biomonitoring of chromium(VI) inhalation exposures that result in internalized lung doses in human subjects.

Keywords: chromium(VI), chromate, lung, magnetic resonance imaging.

Introduction

Magnetic resonance imaging (MRI) is now a dominant imaging modality in clinical medicine. MRI, and the related technique of magnetic resonance spectroscopy (MRS), also provides a novel non-invasive means of acquiring pathomorphological or biochemical data relevant to experimental toxicity studies or toxicity in humans (Deseran *et al*. 1988, Brauer 1993). However, to date, there has been very limited application of MRI to human biomonitoring for biomarkers of exposure or effect, apart from its use in an adjunctive role to other methods (Greger 1999). MRI instruments are now becoming more widespread and it is

* Corresponding author: Andreas Kortenkamp, Centre for Toxicology, The School of Pharmacy, 29–39 Brunswick Square, London, WC1N 1AX, UK. Tel: (+44) 20 7753 5908; Fax: (+44) 20 7753 5908; e-mail: andreas.kortenkamp@ulsop.ac.uk

Biomarkers ISSN 1354-750X print/ISSN 1366-5804 online © 2004 Taylor & Francis Ltd
http://www.tandf.co.uk/journals
DOI: 10.1080/13547500310001659037

likely that the technique has untapped potential in toxicant biomonitoring, particularly for certain metals.

Inhalation exposure to chromium(VI) compounds is associated with lung cancer in humans, as described in a number of epidemiology studies, and certain forms of chromium(VI) are classified as known human carcinogens by the International Agency for Research on Cancer (IARC 1990). Exposure to soluble chromium(VI) compounds occurs in a number of industrial processes such as chrome plating or pigment manufacture, whereas poorly soluble or essentially insoluble compounds such as zinc, strontium, barium or lead chromates are used as paint pigments and anticorrosion agents, and appreciable exposure by inhalation may occur during paint spraying or reworking of surface coating films. It is well established that inhaled particles of sparingly soluble or very slightly soluble chromium(VI) compounds remain in the lung for many years (and that only small amounts of solubilized chromium from these depots reach the bloodstream and other organs (Hyodo *et al*. 1980, Tsuneta *et al.* 1980). Mobilization of chromium(VI) after deposition in the lung is dependent on compound solubility and occurs by: (i) slow solubilization of chromium(VI) in the extracellular fluid and resultant uptake by epithelial cells; and (ii) phagocytosis of chromium(VI) particles by macrophages or epithelial cells with the attendant risk of cytotoxicity or genotoxic damage (Singh *et al.* 1999). The concentration of chromium in lung tissue, normally lower than 1 p.p.m. (wet weight), may reach values in excess of 1000 p.p.m. in occupationally exposed humans as a result of accumulated particles (Kishi *et al.* 1987, Leonard and Bernard 1993). In these circumstances, cytogenetic surveillance is of limited value as a biomarker of internal dose, and it is unsurprising that the analysis of DNA damage in peripheral lymphocytes has yielded equivocal results and is regarded as a poor marker for cancer risk from chromium(VI) inhalation (Kortenkamp 1997). Direct sampling and analysis of lung tissue, or possible alternatives such as pulmonary lavage, are impractical in living subjects, and therefore the need exists for a non-invasive technique to measure the level of deposited chromium in the lung.

This led us to consider whether MRI could be used as a suitable method to determine the chromium lung burden. Intracellular reduction of chromium(VI), predominantly involving glutathione (GSH) and ascorbate as reductants (De Flora and Wetterhahn, 1989), is believed to be crucial to the chromate anion's genotoxicity, although the precise relationship between the various reductive products and the mechanisms of DNA damage has been incompletely established (for a review see Kortenkamp *et al.* 1997, Casadevall and Kortenkamp 2002). Due to an uneven number of outer shell electrons, chromium(III) and certain other chromium species, including chromium(V) and chromium(IV), are paramagnetic and can induce perturbations of the relaxation times of nuclear magnetic resonance (NMR) active nuclei such as ^{1}H (H_2O), ^{13}C and ^{31}P (ATP), which in turn can be visualized using relaxation-weighted magnetic resonance techniques. Various paramagnetic chromium species and their complexes have been probed in biological systems using MRS (Sugiyama 1994, Ueno *et al.* 1995, Liu *et al.* 1997), and chromium(III) complexes can be used as MRI contrast agents (Golman *et al.* 1988). Chromium(VI) itself is non-paramagnetic and therefore MRI 'silent'.

It was hypothesized that MRI could image and locate paramagnetic chromium, including chromium(III), formed during the reductive conversion of chromium(VI) in the lung.

This paper describes preliminary work to determine whether MRI has the necessary sensitivity and selectivity to monitor for the presence of paramagnetic chromium as a biomarker of effective dose *in vitro* and in rat lung. Using a post-mortem rodent model it is shown that the reductive conversion of chromium(VI), and therefore the existence of this toxicant species in the lung, can be indirectly detected by MRI. The ultimate objective of the work is to determine whether MRI could have practical application in human subjects for the biomonitoring of chromium(VI) inhalation exposures and the tracking of persistent and cumulative lung depots of this known carcinogen.

Materials and methods

Chemicals

Potassium chromate was purchased from BDH Ltd (Poole, UK). GSH and ascorbic acid were obtained from Sigma (Poole, UK). Saggital was obtained from Centaur Services Ltd (Castle Cary, UK). Male Wistar rats (bodyweight range 165–340 g) were obtained from Charles River (Margate, UK). The phosphate buffer used was $Na_2HPO_4.2H_2O/NaH_2PO_4.H_2O$, 0.1 M, pH 7.0, and known to be essentially free of any significant contamination by paramagnetic chromium species. Unless otherwise stated, GSH at a standard concentration of 5 mM was used in experiments where chromium(VI) conversion to chromium(III) was required. All experiments were performed at ambient temperature close to 20°C.

MRI instrumentation

All MRI was performed on a VARIAN/Siemens SISCO-200 imaging spectrometer, equipped with an Oxford Instruments 4.7 T, 33 cm horizontal bore superconducting magnet. VARIAN VNMR software was used for MRI scanning, signal processing and image analysis. The instrument parameters given in table 1 were used in all the experimental series. Throughout this paper the terms 'MRI signal' or 'signal' refer to the magnetic resonance signal.

Reaction vials, isolated lungs or whole animals were placed in a purpose-built 62 mm (internal diameter) birdcage-design radio-frequency coil. Reaction vials were scanned in an upright position in the axial plane. Rats were placed into the MRI scanner with their ventral surface uppermost and two-dimensional image slices were acquired in the coronal (ventral to dorsal) plane of section. Consistent placement of animals in the MRI magnetic coil aperture was ensured by a combination of a rigid cradle with limb fixation, anatomical markers, and accurate Z-axis placement within the MRI instrument

Table 1. Parameters used during MRI scans.

Echo time	10 ms
Pulse sequence	Spin-echo sequence
Slice thickness	0.5 mm
In plane spatial resolution	0.625 mm × 0.625 mm
Acquisition time	2 ms
Number of points (real and imaginary)	256
Number of phase encoding steps	128
90° pulse	2 ms gauss
180° pulse	2 ms gauss
G_{read}	20 mT m^{-1}
Maximum G_{phase}	17.92 mT m^{-1}
G_{slice}	36.2 mT m^{-1}
Number of slices	12
Repetition time	0.5 s
Number of repetitions	4
Total imaging time	4 min 26 s

(using a centimetre scale). From the 12 image slices (tomographs) normally obtained for each animal, the typical number of images revealing low signal intensity ('darkfield') was six. The tomograph images with the largest lung darkfield areas were selected for detailed visual assessment and image processing and analysis.

MRI in vitro *experiments*

For the *in vitro* experiments, test solutions were prepared in thin wall glass reaction vials. Phosphate buffer was used as a diluent and also as the negative control. A 0.5 mM chromium(III) solution, prepared by incubating 0.5 mM potassium chromate with 1 mM ascorbate in phosphate buffer for 1 h, provided a reference standard with a known concentration of chromium(III). Reaction mixtures containing chromium(VI) as potassium chromate at 0.05, 0.25 or 0.5 mM in the presence of 5 mM GSH in phosphate buffer were prepared. After thorough mixing and placement of the samples into the radio-frequency coil sample holder, MRI scans were performed on all vials after 0, 5, 10, 15, 30, 60 and 80 min, and thereafter at 60 min intervals, for a total period of 10 h. Densitometry was performed on these MRI images and signal intensities were plotted as arbitrary intensity units.

MRI of post-mortem animal model

Male Wistar rats (bodyweight approximately 250 g) were killed with an overdose of Saggital. After dissection of the neck, a cannula approximately 3 cm in length and 1.5 mm in diameter was introduced midway along the trachea, using a small incision to ensure that the cannula was very tightly fitting. The cannula was then advanced until contact was made with the primary bifurcation of the bronchi. It was then withdrawn a few millimetres and secured by tying around the trachea with suture thread. A length of plastic tubing was attached to the cannula and the animal was placed within the MRI instrument. The lungs were inflated by means of a 10 ml syringe filled with air and the animal was scanned to establish a baseline image of both lungs prior to the introduction of any test solution.

In the experiments involving chromium(III), successive doses (0–15 μg in total, as 2.5 μg/100 μl aliquots in phosphate buffer) were advanced along to the start of the cannula and then instilled by rapid displacement ('burst' instillation) with 5 ml of air from a 10 ml syringe. It was established that this resulted in negligible amounts of test solution remaining in the cannula. The lungs were then re-scanned after each administered dose using identical MRI parameters to those used to obtain the baseline image.

For the experiments using chromium(VI), a baseline MRI image of the lungs was first obtained, and then a single dose of 100 μg chromium(VI) in a volume of 100 μl phosphate buffer was introduced into the right lung only of a Wistar rat (250 g bodyweight) using the burst instillation method described above. The left lung was untreated to provide an internal control for comparison. Both lungs were then re-imaged. The lungs of a second animal were instilled with phosphate buffer and scanned for the same period of time to evaluate the occurrence of any non-specific post-mortem changes.

In all experiments, the total time to complete the MRI scans was 30 min. Experiments were typically repeated three times, using three animals.

Densitometry

In order to determine chromium(III)-induced proton relaxation, the signal intensity of delineated regions within the darkfield region of the lung was measured using densitometry, with the values obtained for the baseline image being subtracted from subsequent images obtained after each successive chromium(III) instillation.

Results

Preliminary in vitro *studies*

Preliminary studies were performed to establish whether the MRI instrument and experimental conditions used could: (i) differentiate between paramagnetic chromium(III) and non-paramagnetic chromium(VI) when present in aqueous solution in a simple test system using reaction vials; and (ii) in the same test system, follow the kinetics of the reductive conversion of chromium(VI) utilizing GSH to model intracellular reductant effects. Chromium(III) alone dissolved in phosphate buffer at a concentration of 0.5 mM was readily detectable and produced a strong signal of approximately 800 intensity units. As shown in figure 1, baseline levels of

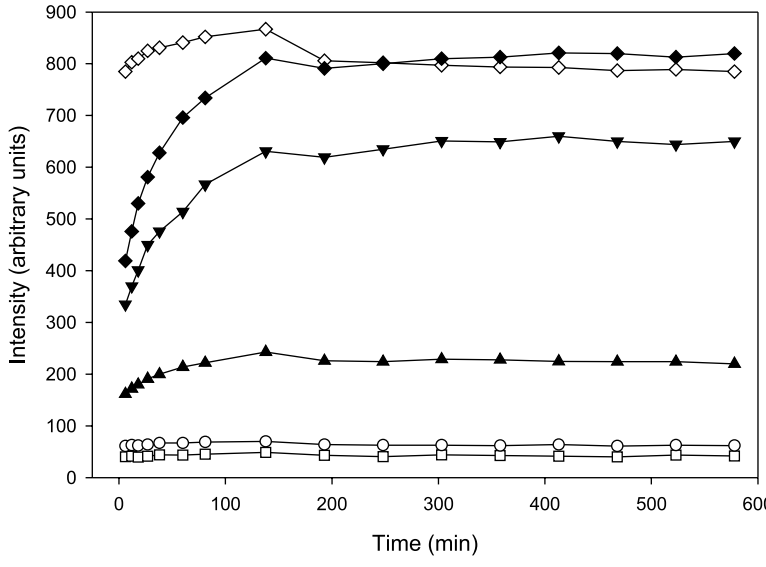

Figure 1. Reduction kinetics of MRI-silent chromium(VI) to MRI-active chromium(III) from a representative experiment. Closed symbols indicate increasing concentrations of chromium(VI) in the presence of 5 mM GSH (▲, 0.05 mM; ▼, 0.25 mM; ◆, 0.5 mM). Open symbols indicate the positive and negative controls (□, phosphate buffer; ○, 0.5 mM chromium(VI); ◇, 0.5 mM chromium(III)).

signal intensity (around 50 units), comparable to the phosphate buffer control, were obtained at all time points for the sample containing 0.5 mM chromium(VI). However, a rapidly developing and concentration-dependent increase in signal intensity was evident when reaction vials containing various concentrations of chromium(VI) (0.05–0.5 mM) were allowed to react with 5 mM GSH. Under the conditions employed, signal strength maxima were detected after a reaction interval of approximately 140 min. The kinetics of the reaction were broadly similar at all concentrations of chromium(VI), with $>80\%$ of the maximal signal intensity being achieved at 60 min. The signal intensity observed for the 0.5 mM chromium(VI)/GSH reaction admixture was comparable to that of the 0.5 mM chromium(III) sample (figure 1).

Studies using a post-mortem model

The above studies demonstrated the potential of MRI for the detection of paramagnetic forms of chromium, including chromium(III), in an *in vitro* non-biological system. Attention was then focused on the application of this method to monitor for the presence of a smaller amount of instilled chromium(III) or chromium(VI) to model doses more applicable to human inhalation exposures. The primary areas of focus in these experiments were: (i) the examination of the sensitivity of this technique with the lungs left *in situ* in a whole animal; (ii) the determination of whether the reduction of chromium(VI), and therefore its presence, could be followed under such circumstances; (iii) the assessment of inter-subject variation; and (iv) the optimization of the image analysis methodology applied to the MRI lung images.

Incremental doses of chromium(III) were instilled into the lungs (0–15 μg as successive 2.5 μg aliquots) and MRI scans taken after each administered dose. The experiment was repeated three times, using a total of three animals. Figure 2a shows the MRI tomographs generated over the range of chromium(III) doses (0–15 μg) during a representative experiment on a single animal. The boxes highlighted on the 15 μg image represent the regions of interest within which densitometry was performed. It can be clearly seen that there is an increase in the recorded signal intensity in the central region of each lung that is proportionate to the total amount of administered chromium(III). When these changes were quantified by image analysis a linear rise in signal intensity was evident – in this case, over the dose range of 2.5–10 μg (figure 2b). By means of image analysis, differential intensity levels of up to 60 units versus the control were seen at the highest dose of chromium(III) used (15 μg), although increases were routinely detectable with 5.0 μg chromium(III). In some cases, visual assessment of images provided evidence of relatively small foci of elevated signal intensity within one (for example see figure 2a) or both lung lobes. A range of 2.5–5 μg chromium(III) was considered to be the lower limit of detection under these experimental conditions.

To control for effects such as the extent of lung inflation, the influence of vehicle buffer instillation or post-mortem changes in the lung tissue, parallel studies were conducted with animals where equivalent volumes of phosphate buffer alone were incrementally instilled into the lungs over the same timeframe. No changes in signal intensity or any other notable alterations in MRI images were apparent at any time point up to 6 h in these controls (data not shown).

Monitoring the conversion of chromium(VI) to chromium(III) in situ *in the lung*

Having established a sensitivity threshold for the detection of chromium(III), studies were then performed to assess whether it was possible to monitor the conversion of chromium(VI) ultimately to chromium(III) as a result of the reducing capacity of the internal environment of the lung – thus providing a biomarker for the presence of chromium(VI). The same whole animal model was used with the exception that a single dose of 100 μg of chromium(VI) as potassium chromate was introduced into the right lung of a freshly killed male Wistar rat (250 g); the left lung was untreated to provide a contralateral comparator. Scans were performed at 10 min intervals up to 30 min after dose instillation. Ten minutes after introduction of chromium(VI) into the right lung, confluent areas of elevated signal amplitude concentrated in the upper third of the lung were detected. The experiment was repeated three times; representative results are shown in figure 3a. Further signal intensification occurred up to 30 min. No changes were visible in the untreated left lung.

Densitometric analysis confirmed the early rise in signal in the chromium(VI) treated-lung and the absence of any effect in the untreated lung (figure 3b). In this particular experiment, the maximum signal amplitude was evident after approximately 30 min and corresponded to 80 intensity units. In the contralateral untreated lung, baseline values of around 20 intensity units are seen over the total time period. MRI scans conducted over an equivalent time period on animals

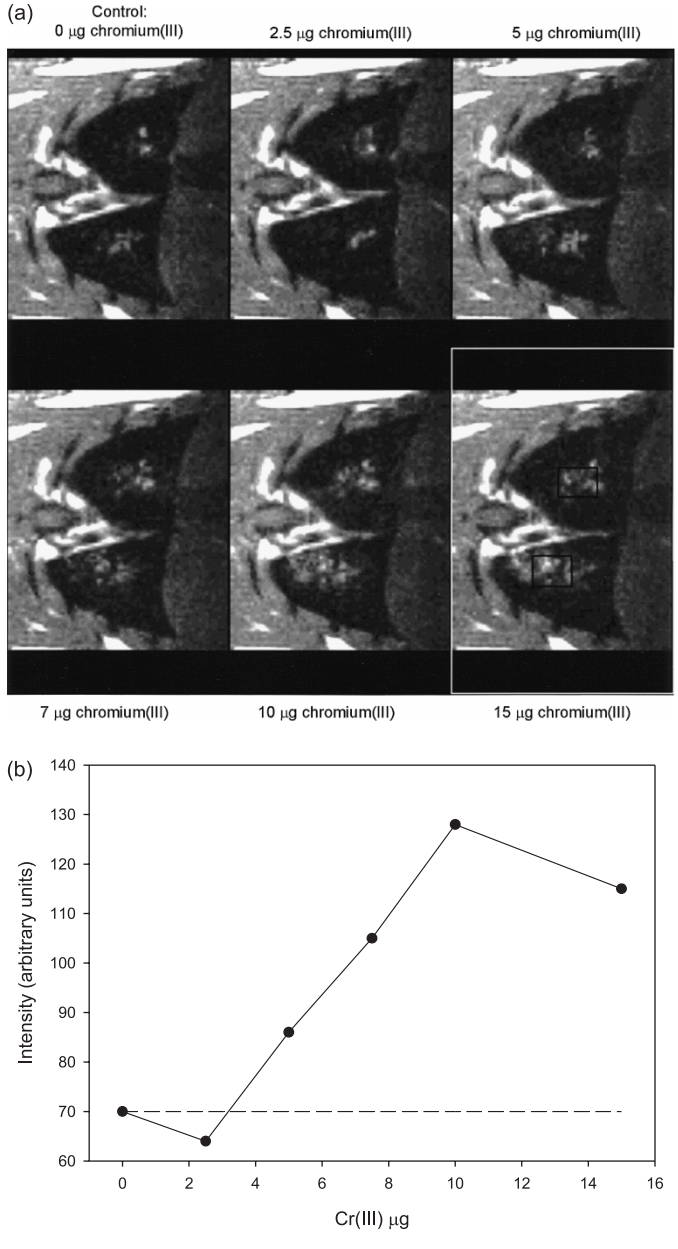

Figure 2. Imaging of chromium(III) deposited in the lungs of a post-mortem rat model. (a) MRI scans of post-mortem rat lung showing changes in signal intensity with incremental instillation of 0, 2.5, 5, 7, 10 and 15 μg of chromium(III). (b) Quantification of MRI signal intensity with increasing dose of chromium(III). Densitometry was carried out on selected regions of the images shown in figure 2a, and a plot constructed of the signal intensity of both lungs (arbitrary units) versus administered chromium(III) dose. The signal intensity values obtained for the baseline image of all animals were subtracted from the subsequent images obtained after each successive chromium(III) instillation. In both (a) and (b) the results shown are from a single representative experiment involving one animal.

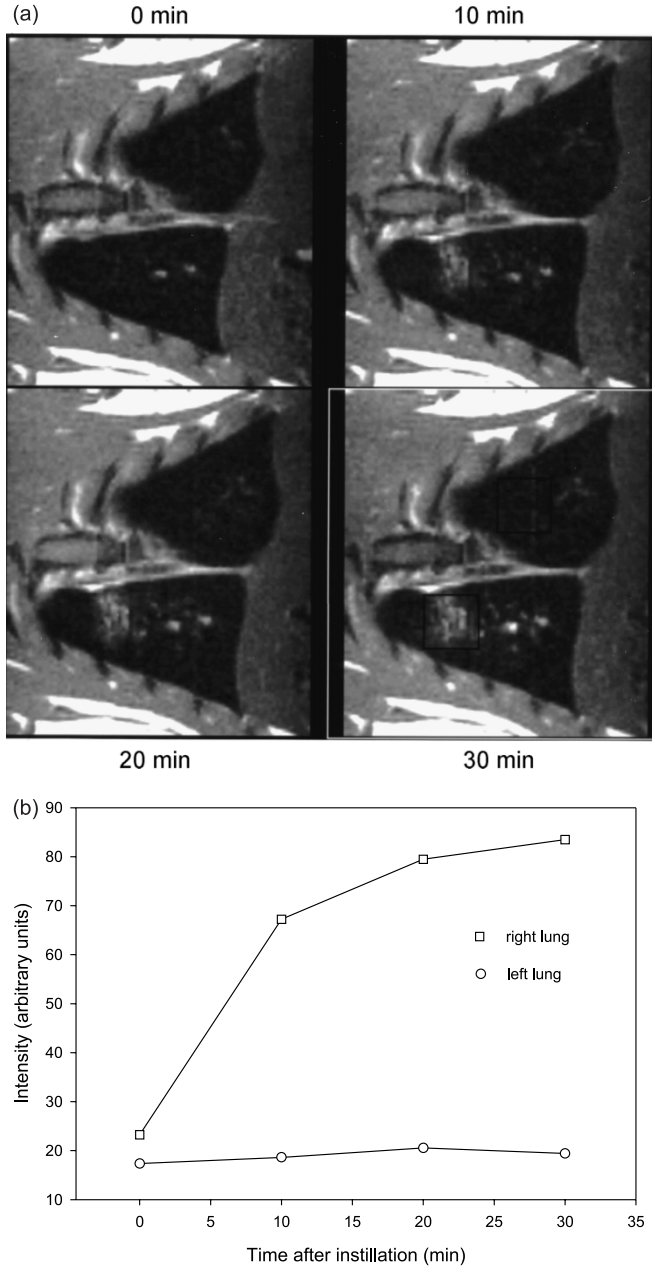

Figure 3. Visualization of the reductive conversion of chromium(VI) in a post-mortem rat lung model. (a) MRI scan after installation of a single dose of 100 μg chromium(VI) in phosphate buffer. Scans were carried out 0, 10, 20 and 30 min after instillation. Chromium(VI) was introduced into the right lung only (bottom), with the left lung (top) remaining untreated. (b) Quantification of MRI signal intensity during the conversion of chromium(VI) to chromium(III). Densitometry was carried out on selected regions of the lung images shown in figure 3a, and a plot constructed of the signal intensity (arbitrary units) versus time. In both (a) and (b) the results shown are from a single representative experiment.

treated with 100 μl of phosphate buffer alone revealed no detectable changes (data not shown).

Image analysis techniques

The image analysis software used in the initial experiments was configured to calculate the average intensity over a defined region of interest manually designated on the basis of an initial visual assessment of the MRI images. During repeat experiments (to scale up the size of the experimental groups) it was noted that chromium treatment could produce changes that were dispersed throughout the whole lung region. In order to determine the impact of varying the mode of analysis of signal intensity, the results of the previous experiments (figure 2a) were recomputed with the whole darkfield area of the lungs delineated as the area for analysis. The quantified level of signal intensity in these images was found to be essentially the same irrespective of whether the whole lung or a more select region of interest was delineated for analysis (figure 4). For all subsequent studies image analysis was standardized using the method involving signal intensity determination for the whole lung area.

Quantification of the chromium(III) MRI signal

A series of experiments was designed to explore inter-animal variations in MRI image characteristics following administration of a standardized amount of chromium(III) and to quantify the associated changes in signal intensity. A group of three rats were scanned to obtain baseline images and then dosed with 30 μg chromium(III). Figure 5 shows pairs of images (pre-dose control and post-dose at 30 min) obtained from individual animals. With this relatively high amount of

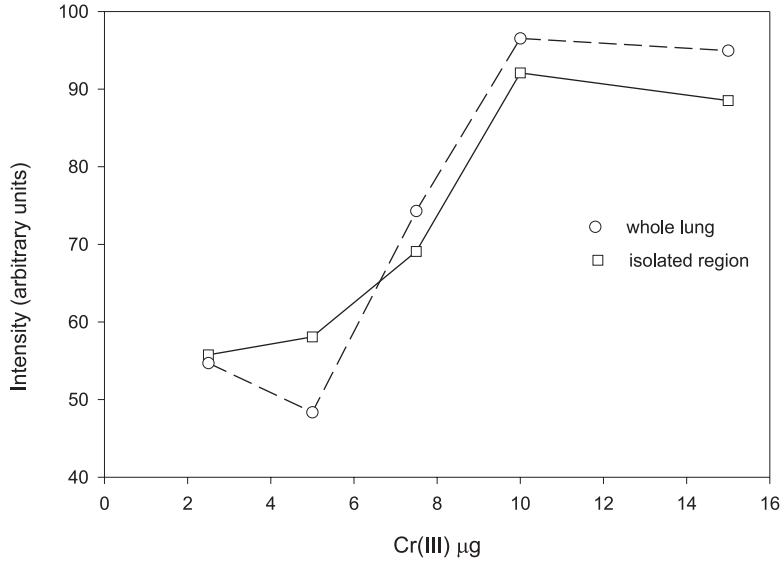

Figure 4. Recomputation of image analysis signal intensity using different lung area delineation techniques. The images shown in figure 2a were re-analysed by densitometry using either a visually selected region of interest or whole lung area integration.

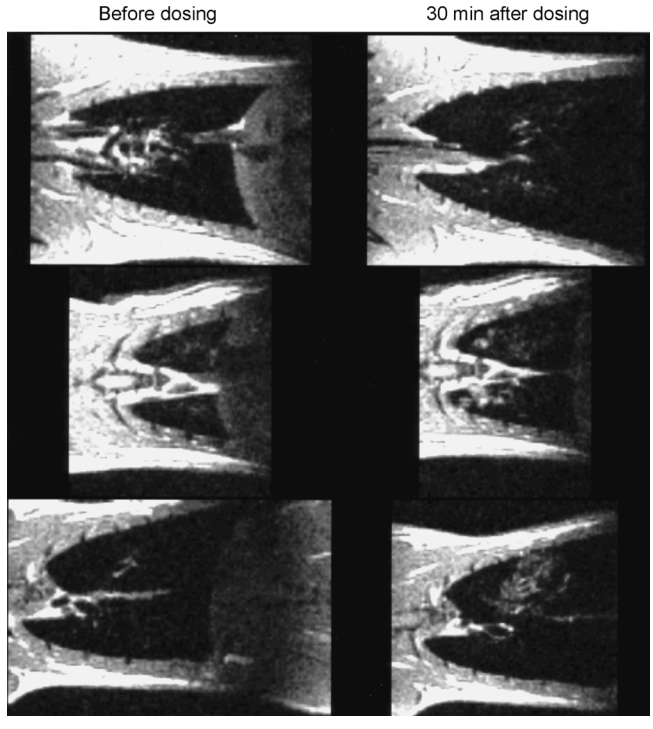

Figure 5. Comparison of MRI scans before and after dosing with 30 μg of chromium(III) in the lungs of three different rats post mortem. Top row, animal 1; middle row, animal 2; bottom row, animal 3 (numbering as in table 2).

chromium(III), large confluent areas of increased signal intensity were readily seen in the lung darkfield. Image analysis by densitometry was performed on the pre- and post-dose image pairs, and the pre-dosing baseline image signal intensities (averaged over both lungs) were subtracted from the post-dosing equivalents to determine the net intensity difference (table 2). In all but one case, increased signal intensities could be confirmed by image analysis.

Discussion

Initial experiments *in vitro* demonstrated that, with our chosen MRI parameters, paramagnetic chromium(III) in aqueous solution could be readily detected,

Table 2. Inter-animal variation in the MRI signal intensity change determined for the total lung region after administration of 30 μg chromium(III).

			Total intensity		
Animal no.	Weight (g)	Chromium(III) dose (μg)	Post-dosing	Baseline	Net change in intensity
1	340	30	2669	5713	−3044
2	320	30	8235	1399	6836
3	320	30	6519	2144	4375

Animals are numbered as in figure 5.

and also confirmed that chromium(VI) was paramagnetically silent until reduced to paramagnetic chromium forms (figure 1). GSH was used for the reductive conversion since, along with ascorbate, it is a key intracellular reductant present at millimolar concentrations in the cytosol and is involved in the production of genotoxic chromium species, as was borne out by our *in vitro* studies (figure 1). Within simple *in vitro* systems at neutral pH, the reaction of GSH with chromium(VI) results in significant formation of chromium(V)–GSH intermediates (O'Brien *et al.* 1985), and even normally very transient chromium(IV) forms may be more stable in these circumstances (Liu *et al.* 1997). These species are known to be paramagnetic, and in the experiments reported here, chromium(V) and possibly also chromium(IV) would be expected to have influenced magnetic resonance relaxation, in addition to the substantial contribution predicted from chromium(III) formation.

Subsequent investigations centred on whether MRI could detect small amounts of chromium(III) as an endpoint biomarker for internalized doses of chromium(VI) when present in lungs within whole animals. The quantities chosen for instillation were designed to be relevant to lung doses in human exposure to chromium compounds. A typical occupational exposure limit norm for chromium(VI) in a number of industrialized countries is 50 μg m^{-3}, as an 8 h time-weighted average (ACGIH 1999, DFG 1999), although in some cases lower limits have been established for insoluble chromium(VI) species (ACGIH 1999). This order of airborne chromium(VI) concentration when modelled as a rat inhalation exposure equates to a theoretical total lung deposition of approximately 5 μg (assuming a minute volume of 0.22 l and therefore a total air exchange volume of approximately 100 l over 8 h). Thus it was considered that a lung total dose of 5 μg was appropriate as a benchmark in consideration of the required chromium(III) detection limit. When seen in the context of typical human exposures, this obviously represents a very simplified acute model since it does not take into account elimination or accumulation processes in the lung, or all the complex dynamics of the chromium(VI) reduction process. It is also necessary to consider some other limitations of the approach used in these initial modelling experiments. An instillation technique rather than inhalation exposure was used for dose delivery, and it is acknowledged that, even with diffusion effects, this resulted in the concentration of the dose in more limited regions of the lung than would have been expected with inhalation exposure. Furthermore, the dosing method may have resulted in unequal dose deposition to each lung. Euthanized animals were selected as the model to avoid any methodological complications arising from the influence of respiratory movements on MRI scanning.

It was ascertained that a lung depot of 5 μg chromium(III) was readily detectable in the rat lung using MRI by visual assessment or semi-quantitative image analysis (figure 2). In some animals a dose of 2.5 μg produced a signal that was considered to be above the baseline control. It is possible that this variability in the limit of detection simply resulted from inter-individual differences in the delivery pattern of the burst instillation technique employed. However, it was considered that within the constraints of the experimental conditions, MRI was capable of providing the required order of detection sensitivity for chromium(III).

Incremental instillations of chromium(III) made in single animals caused linear or near-linear increases in signal strength with cumulative dose when lung regions selected by visual assessment were subjected to image analysis (figure 2b).

The possibility that non-specific changes were occurring simply as a result of introducing fluid into the lung, or due to lung hyperinflation, was eliminated in a series of control experiments where phosphate buffer instillation failed to cause any detectable increase in signal intensity when monitored for up to 6 h. This conclusion was supported by the finding that control images of the lungs showed negligible variations irrespective of whether only air or phosphate buffer was introduced. Although post-mortem changes such as tissue autolysis and accumulation of tissue fluid in the lungs might be postulated to have an effect on MRI images, no discernible effects were observed in the controls even several hours after death. Similar considerations lead us to rule out possible confounding effects through the formation of localized oedema by chromium(VI), which could have led to increases in MRI signal intensity. Although chromium(VI) is a well-known respiratory irritant, such effects would not have occurred within the time frame of our experiments. The patterns of signal density obtained over several hours after chromium(III) instillation showed only small variations, which may have been due to either local diffusion and dilution events, or to effects on ^{1}H magnetic relaxation time arising from the reaction of chromium(III) with proteins – as described by Barnhart and Berk (1986) – or other macromolecules.

From the viewpoint of application to the biomonitoring of inhaled chromium(VI), it was of fundamental importance that conversion of this MRI 'silent' form of chromium could be imaged under conditions where lungs in whole animals were being scanned. A readily soluble chromium(VI) compound was used at a comparatively high dose level since only a single exposure over a short-term period was to be followed. One striking feature of these experiments was the rapidity and magnitude of the increase in signal intensity after chromium(VI) instillation into the lung (figure 3). In common with the *in vitro* studies discussed previously, we could not quantify the relative contribution of the signal arising from the formation of the various possible paramagnetic chromium species, but it was noted that an essentially stable image was achieved by the 30 min time point. It is plausible that chromium(VI) reduction took place in both the extracellular and the intracellular environment, since it is known that the pulmonary epithelial lining fluid in a number of species, including rats and humans, contains significant amounts of antioxidants, including GSH and ascorbate (Slade *et al.* 1993). These would constitute immediately available extracellular reducing equivalents. Based on *in vitro* studies with ultrafiltrate and cytosolic preparations, Standeven and Wetterhahn (1992) proposed that ascorbate is actually the principal reductant of chromium(VI) in the rat lung. It would be logical to repeat this work using subchronic inhalation exposures to a lower solubility chromate to investigate whether cumulative lung deposition could be monitored in animals sacrificed at various study time points.

Quantification of signal intensities was limited by the resolving power of the image analysis software used for the densitometric measurements, which was not optimized to detect the subtle changes in signal intensity that occurred after the

introduction of small amounts of chromium. Preliminary evaluations of image densitometry techniques to ascertain whether signal averaging over the whole lung or a region of altered brightness was more sensitive produced encouraging results (figure 4). In larger scale experiments, where moderately high chromium(III) doses of 30 μg were introduced as a single instillation into the lungs of a group of rats, visual assessment of images appeared to show qualitatively significant increases in signal intensity (figure 5), which could in all but one case be unequivocally quantified when images were subjected to densitometric image analysis (table 2). The paradoxical image analysis results with one animal are attributed to difficulties with distinguishing thoracic structures from areas with increased brightness due to chromium(III).

The development of the MRI technique described in this paper may have promise for lung biomonitoring of humans exposed to chromium compounds, and in particular the visualization of poorly soluble chromium(VI) depots, which are difficult to detect using conventional biomonitoring methods. Once chromium(VI) compounds have entered the cell and have undergone reductive conversion, the resulting chromium(III) complexes are known to be relatively stable and therefore their persistent paramagnetic modification of the magnetic resonance signal decay constants T_1 (spin-lattice) and T_2 (spin-spin) should mean that, by selecting appropriate MRI parameters, regions of tissue containing chromium(III) can be visualized as areas of increased brightness. Although, in common with urinary or plasma chromium measurements, this is an indirect chromium(VI) detection method, it has the distinct advantage of allowing monitoring of the lung, since this is the target organ in chromium(VI) carcinogenicity. Another valuable aspect of MRI is that it enables acquisition of a series of contiguous image slices through a tissue, so that the image set covers and is representative of the entire tissue. Lung structure imaging by conventional MRI is technically difficult since the signal from lung parenchyma is limited due to a low proton density and multi-exponential relaxation times, amongst other factors (Bergin *et al.* 1993). However, this is actually beneficial in this instance since the background low magnetic resonance signal from the lung parenchyma provides darkfield contrast, thereby facilitating the identification of chromium depots.

It is envisaged that, in a manner analogous to pre-employment lung function testing, workers could undergo baseline MRI scans prior to chromium exposure, and then subsequently be scanned at intervals to determine their chromium lung load status. At this early stage it is not possible to determine whether the technique could be successfully used in a fully quantitative manner. Furthermore, there are other practical considerations and limitations. For example, use in living subjects would necessitate that the effects of breathing motion be excluded, for example by means of rapid chest scanning during breath-holding. The underlying principle of the technique also may limit its application in certain occupational environments, in particular those where ferromagnetic particle confounding could occur. Magnetic lung-retained contaminants produce measurable magnetic moments in exposed humans (Kalliomäki *et al.* 1981), which would be expected to swamp any paramagnetic signal from collateral chromium lung depots. This is likely to be a limitation with regard to stainless steel welding or foundry atmospheres.

To our knowledge, this study utilizing T_1-weighted proton (^{1}H)-MRI is the first reported attempt to assess the potential of MRI for chromium biomonitoring. Aside from routine biomonitoring applications, it could also serve as a research tool to allow levels of chromium(VI)-containing particles in the lung to be quantified and correlated with chromium levels in body fluids or biological effect markers. The basis of the detection method is directly linked to the reductive conversion of chromium(VI) *in situ*, which results in this agent's carcinogenic hazard. Therefore it can be seen as a biomarker of biologically effective dose, and may provide a basis for an alternative to cytogenetic studies in non-lung tissues. Together with what is already known about chromium toxicokinetics and genotoxic mechanisms, MRI information about the deposition and persistence of chromium(VI) compounds in the lung has the potential to integrate the assessment of carcinogenic risk to exposed individuals.

Acknowledgements

The NMR imaging spectrometer was provided by the University of London Intercollegiate Research Service scheme and was located at Queen Mary, University of London. Rob Shayer is grateful for support by Ford Motor Company.

References

ACGIH. 1999, *TLVs® and BEIs®*. Cincinnati: American Conference of Governmental Industrial Hygienists. Cincinnati, USA

Barnhart, J. L. and Berk, R. N. 1986, Influence of paramagnetic ions and pH on proton NMR relaxation of biologic fluids. *Investigative Radiology*, **21**, 132–136.

Bergin, C. J., Glover, G. M. and Pauly, J. 1993, Magnetic resonance imaging of the lung parenchyma. *Journal of Thoracic Imaging*, **8**, 12–17.

Brauer, M. 1993, Magnetic resonance imaging and spectroscopy: new noninvasive *in vivo* approaches in toxicology research. *Alternatives to Laboratory Animals*, **21**, 411–425.

Casadevall, M. and Kortenkamp, A. 2002, Chromium and cancer. In *Heavy Metals in the Environment*, edited by B. Sarkar (New York, Basel: Marcel Dekker New York), pp. 271–308.

De Flora, S. and Wetterhahn, K. E. 1989, Mechanisms of chromium metabolism and genotoxicity. *Life Chemistry Reports*, **7**, 169–244.

Deseran, M. W., Colletti, P. M., Ratto, D., Ansari, A. and Siegel, M. E. 1988, Chronic berylliosis. Demonstration by gallium-67 imaging and magnetic resonance imaging. *Clinical Nuclear Medicine*, **13**, 509–511.

DFG (Deutsche Forschungsgemeinschaft). 1999, *List of MAK and BAT Values* 1999, *Commission for the Investigation of Health Hazards of Chemical Compounds in the Work Area, Report No. 35*. Weinheim: Wiley-VCH.

Golman, K., Klaveness, J., Holtz, E., Leunbach, I., Rye, A. S. and Almen, T. 1988, A magnetic resonance imaging contrast medium for the liver and bile. *Investigative Radiology*, **23** (Supplement 1), 243–245.

Greger, J. L. 1999, Nutrition versus toxicology of manganese in humans: evaluation of potential biomarkers. *Neurotoxicology*, **20**, 205–212.

Hyodo, K., Suzuki, S., Furuya, N. and Meshizuka, K. 1980, An analysis of chromium, copper and zinc in organs of a chromate worker. *International Archives of Occupational and Environmental Health*, **46**, 141–150.

IARC. 1990, *Monographs on the Evaluation of the Carcinogenic Risk of Chemicals to Humans*, *Vol. 49, Chromium, Nickel and Welding* (Lyon: International Agency for Research on Cancer).

Kalliomäki, K., Aittoniemi, K., Kalliomäki, P.-L. and Moilanen, M. 1981, Measurement of lung-retained contaminants *in vivo* amongst workers exposed to metal aerosols. *American Industrial Hygiene Association Journal*, **42**, 234–238.

Kishi, R., Tarumi, T., Uchino, E. and Miyake, H. 1987, Chromium content of organs of chromate workers with lung cancer. *American Journal of Industrial Medicine*, **11**, 67–74.

Kortenkamp, A. 1997, Problems in the biological monitoring of chromium(VI) exposed individuals. *Biomarkers*, **2**, 73–80.

KORTENKAMP, A., CASADEVALL, M., DA CRUZ FRESCO, P. and SHAYER, R. O. J. 1997, Pathways in the chromium(VI)-mediated formation of DNA lesions: a review. *NATO ASI Series*, **2**, 15–34.

LEONARD, A. and BERNARD, A. 1993, Biomonitoring exposure to metal compounds with carcinogenic properties. *Environmental Health Perspectives*, **101** (Supplement 3), 127–133.

LIU, K. J., SHI, X. and DALAL, N. S. 1997, Synthesis of Cr(IV)-GSH, its identification and its free hydroxyl radical generation: a model compound for Cr(VI) carcinogenicity. *Biochemical and Biophysical Research Communications*, **235**, 54–58.

O'BRIEN, P., BARRETT, J. and SWANSON, F. 1985, Chromium(V) can be generated in the reduction of chromium(VI) by glutathione. *Inorganica Chimica Acta*, **108**, L19.

SINGH, J., PRITCHARD, D. E., CARLISLE, D. L., MCLEAN, J. A., MONTASER, A., ORENSTEIN, J. M. and PATIERNO, S. R. 1999, Internalization of carcinogenic lead chromate particles by cultured normal human lung epithelial cells: formation of intracellular lead-inclusion bodies and induction of apoptosis. *Toxicology and Applied Pharmacology*, **161**, 240–248.

SLADE, R., CRISSMAN, K., NORWOOD, J. and HATCH, G. 1993, Comparison of antioxidant substances in bronchoalveolar lavage cells and fluid from humans, guinea pigs, and rats. *Experimental Lung Research*, **19**, 469–484.

STANDEVEN, A. M. and WETTERHAHN, K. E. 1992, Ascorbate is the principal reductant of chromium(VI) in rat lung ultrafiltrates and cytosols, and mediates chromium-DNA binding *in vitro*. *Carcinogenesis*, **13**, 1319–1324.

SUGIYAMA, M. 1994, Role of paramagnetic chromium in chromium(VI)-induced damage in cultured mammalian cells. *Environmental Health Perspectives*, **102** (Supplement 3), 31–33.

TSUNETA, Y., OHSAKI, Y., KIMURA, K., MIKAMI, H., ABE, S. and MURAO, M. 1980, Chromium content of lungs of chromate workers with lung cancer. *Thorax*, **35**, 294–297.

UENO, S., SUSA, N., FURUKAWA, Y. and SUGIYAMA, M. 1995, Formation of paramagnetic chromium in liver of mice treated with dichromate(VI). *Toxicology and Applied Pharmacology*, **135**, 165–171.